SUPPLEMENTARY TABLES

Supp. Table S1. Mitochondrial respiratory chain enzyme activities in tissues of individuals

	Fibroblasts				Muscle		
	I1 (mUnit/Unit CS)	I2 (mUnit/Unit CS)	I3 (mUnit/Unit CS)	I4 (mUnit/mg protein)	I3 (mUnit/Unit CS)	I4 (mUnit/mg protein)	I6 (mUnit/mg protein)
Complex I	160 (40-120)	236 (163-599)	357 (163-599)	0.20 (0.04-0.12)	89 (47-154)	**13 (40-95)**	n.d.
Complex I + III	52 (23-53)	n.d.	n.d.	1.08 (0.23-0.53)	n.d.	n.d.	**0.43 (0.50-1.90**)
Complex II	27 (18-43)	398 (335-888)	493 (335-888)	0.37 (0.18-0.43)	155 (134-354)		n.d.
Complex III	256 (72-223)	610 (570-1383)	817 (570-1383)	2.89 (0.72-2.23)	799 (696-1756)	**496 (925-2068)**	n.d.
Complex II + III	73 (29-69)	254 (128-534)	254 (128-534)	0.84 (0.29-0.69)	**171 (176-492)**		n.d.
Complex IV	97 (90-179)	461 (288-954)	516 (288-954)	0.47 (0.90-1.79)	616 (470-1842)	**330 (418-1201)**	n.d.
Complex V	105 (39-79)	492 (193-819)	568 (193-819)	1.15 (0.39-0.79)	474 (161-711)	**112 (165-414)**	n.d.

Abnormal results in bold, (reference values).

Supp. Table S2. In silico predictions of missense variants and frequencies in public databases

family, individual, gender, consanguinity	F1, I1, female, no	F2, I2, male, no F2, I3, male, no	F3, I4, female, no	F4, I5, male, yes	F5, I6, female, no
Allel 1	c.91-8725_348+27113 del36096	c.797del	c.231C>G	c.532G>C	c.134G>T
Predicted AA change	p.Lys31_Glndel116	p.Pro266Argfs*10	p.His77Gln	p.Val178Leu	p.Gly45Val
Mutation type	deletion	frameshift	missense	missense	Missense
Mutation Taster score			> 0.999	> 0.999	> 0.999
Mutation Taster prediction			disease causing	disease causing	disease causing
SIFT score			0.000	0.005	0.002
SIFT prediction*			damaging	damaging	Damaging
Provean score			-7.22	-2.74	-8.13
Provean prediction*			deleterious	deleterious	Deleterious
PolyPhen-2 score			1	0.998	1
PolyPhen-2 prediction			probably damaging	probably damaging	probably damaging
Frequency in gnomAD	not listed	4.07e-5	1.22e-5	not listed	not listed
Allel 2	c.1045G>C	c.938A>T	c.1054G>A	homozygous	c.938A>T
Predicted AA change	p.Val349Leu	p.Lys313met	p.Glu352Lys		p.Lys313Met
Mutation type	missense	missense	missense		Missense
Mutation Taster score	> 0.999	> 0.999	> 0.999		> 0.999
Mutation Taster prediction	disease causing	disease causing	disease causing		disease causing
SIFT score	0.127	0.210	0.057		0.210
SIFT prediction*	tolerated	tolerated	tolerated		Tolerated
Provean score	-1.26	-2.98	-3.43		-2.98
Provean prediction*	neutral	deleterious	deleterious		Deleterious
PolyPhen-2 score	0.167	0.708	0.609		0.708
PolyPhen-2 prediction	benign	possibly damaging	possibly damaging		possibly damaging
Frequency in gnomAD	8.127e-6	0.0001407	9.029e-5		0.0001407

AA = amino acid, *(cutoff=0.05)

Supp. Table S3

Sequences of primers for PCR and sequence analysis, and of hybridization probes for Northern blotting

Region of interest	**Forward 5'->3'**	**Reverse 5'->3'**
Primers PCR genomic DNA		
Exon 6 of *WARS2*	tgtaaaacgacggccagtATTGCAAGTTGGGAACTGTCTG	caggaaacagctatgaccGTCGTATTTCAAAGCTACAAAGC
Primers sequence PCR		
M13 tail	tgtaaaacgacggccagt	Caggaaacagctatgacc
Primers for generation of templates for in vitro transcription		
$tRNA^{Arg}$	AAGGATTAGACTGAACCGA	GCTAATACGACTCACTATAAGAAGTGAGATGGTAAATGC
$tRNA^{Trp}$	GCTACTCCTACCTATCTCCCC	GCTAATACGACTCACTATAGGGGTTTTGCAGTCCTTAG

SUPPLEMENTARY FIGURES

Supp. Figure S1. Modeling of the individual WARS2 variants shown in Fig. 3

Figure S1-A

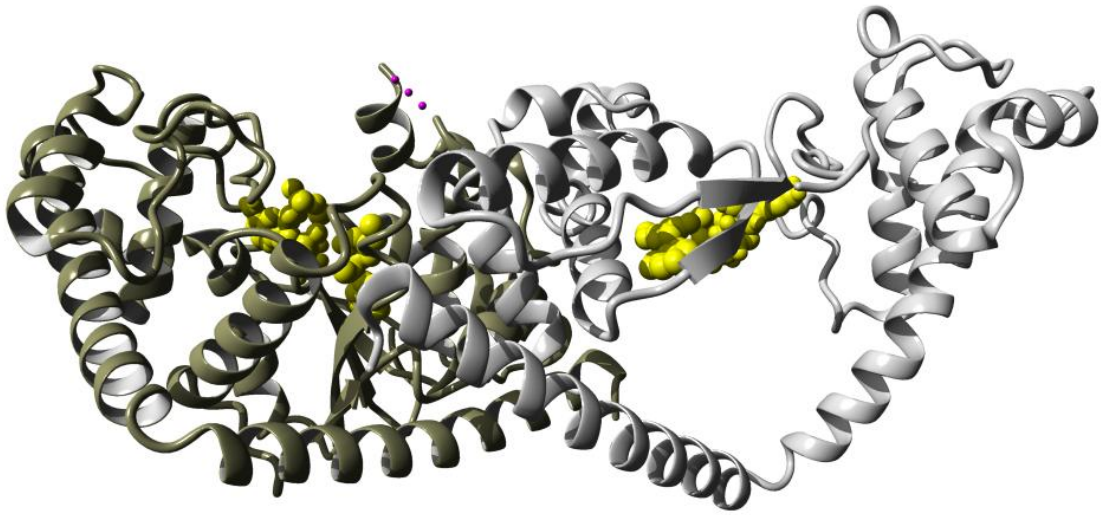

p.Lys31_Q116del

The deletion p.Lys31_Q116del removes part of the stable core of the enzyme. This variant (if expressed) will result in a non-functional protein because it lacks part of the domain where the tRNA and Trp bind.

Supp. Figure S1-B

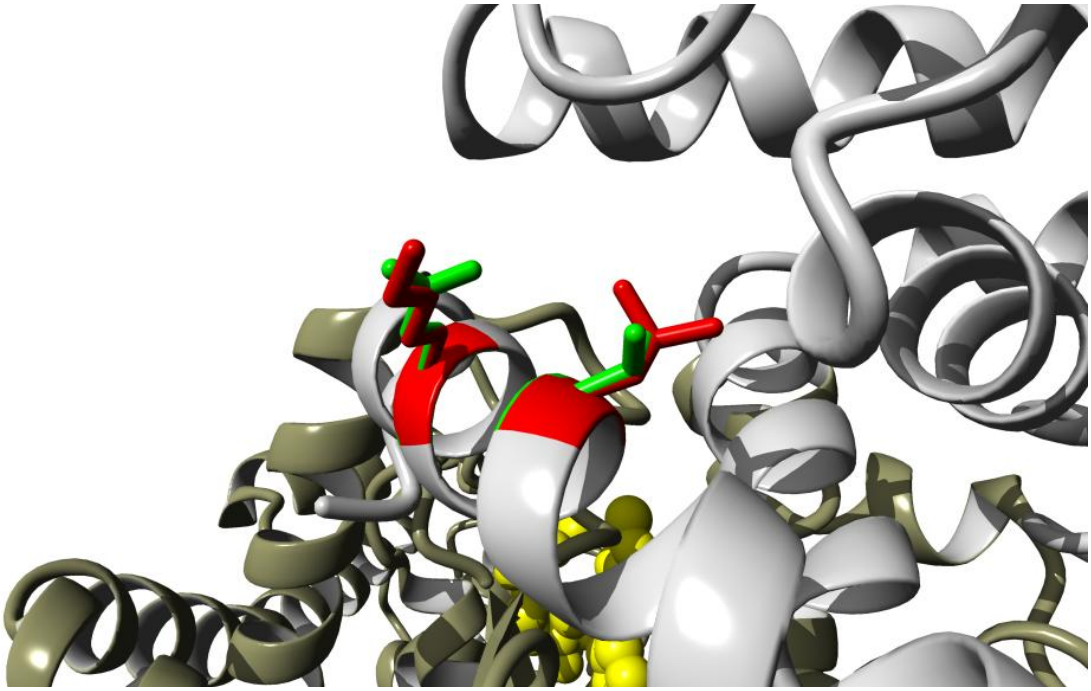

p.Glu352Lys and p.Val349Leu

These two variants are located in the same alpha helix. The p.Glu352 residue normally interacts with p.Lys355, which stabilizes the alpha helical structure of this part of the protein. The variant p.Glu352Lys will interfere with this interaction and therefore destabilize the helical structure of this part of the protein. The p.Val349Leu variant will lead to slight changes in the hydrophobic interactions near the surface of the protein.

Supp. Figure S1-C

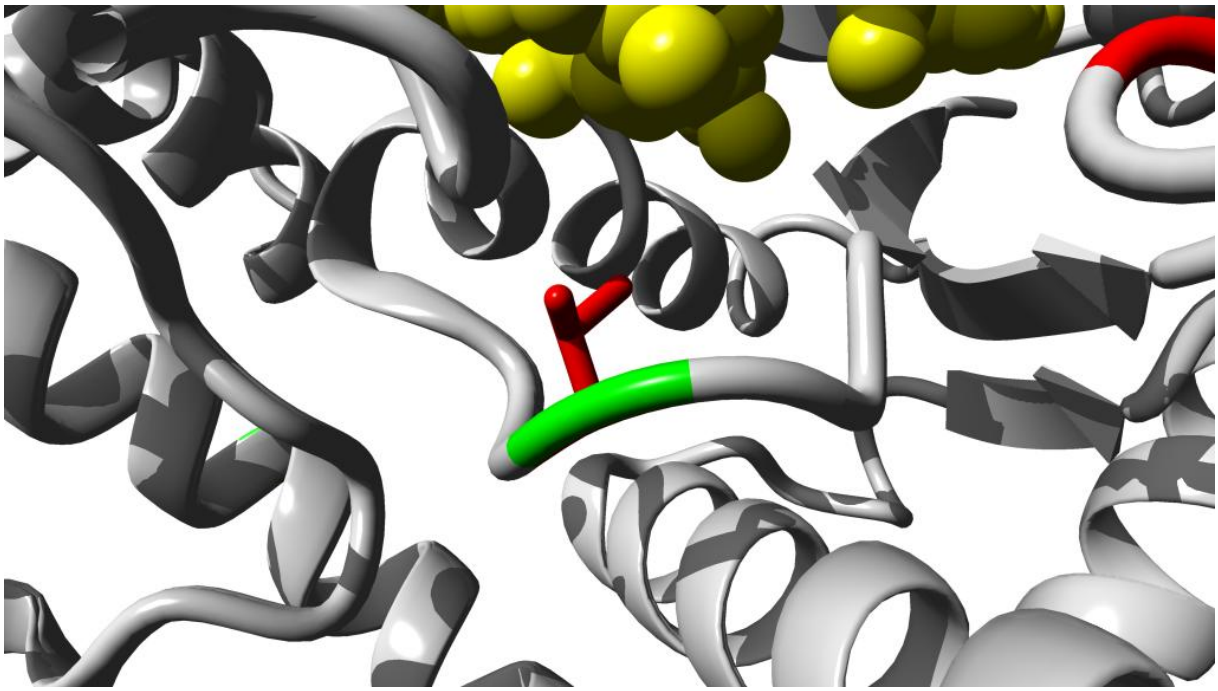

p.Gly45Val

The p.Gly45Val residue is located in a small loop that covers part of the tRNA binding site. The introduction of a larger residue is expected to change the position of the surrounding side chains, which will lead to a change of the tRNA binding, and therefore may interfere with the enzymatic function of the protein.

Supp. Figure S1-D

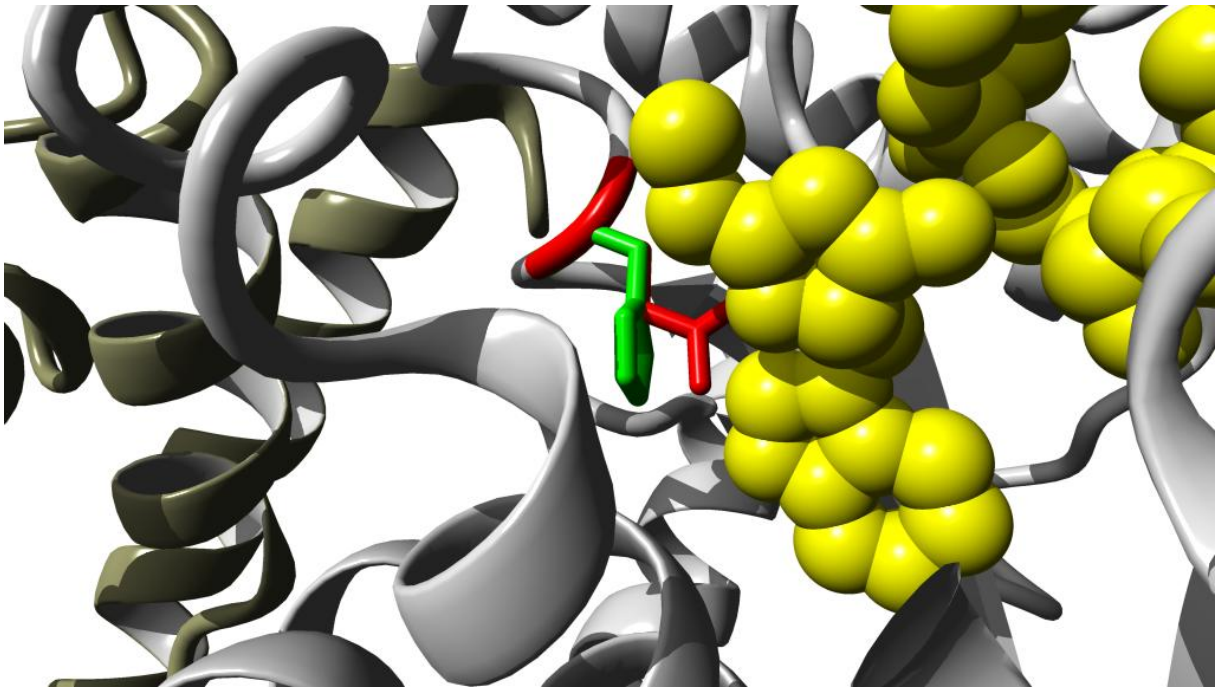

p.His77Gln

This variant is located adjacent to the active site of the enzyme. The p.His77 residue forms a hydrogen bond with p.Asp167 in the nearby alpha helix. The variant p.His77Gln may still allow for thus hydrogen bonding, however, the altered shape and electron density are expected to interfere with ligand binding.

Supp. Figure S1-E

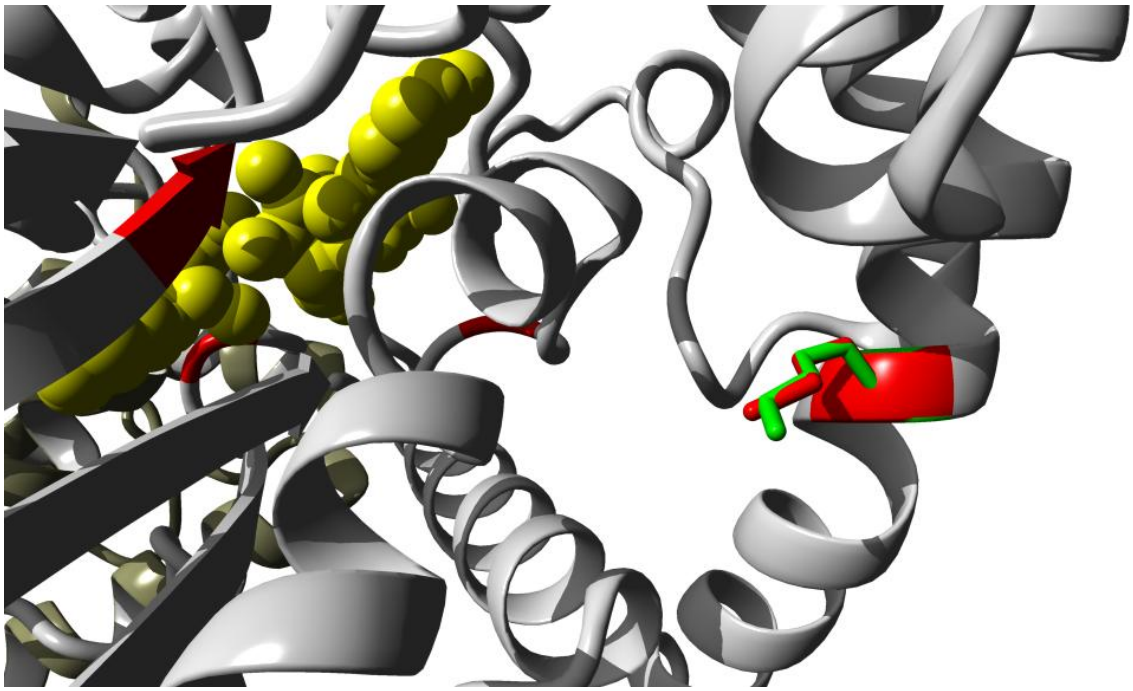

p.Lys313Met

The p.Lys313Met variant is located in a helix consisting of a stretch of conserved residues within the anti-codon recognition domain (Yang, et al., 2006), and changes a positively charged side chain into a hydrophobic side chain. The mutation possibly disturbs an ionic interaction needed for the correct tertiary structure of the enzyme required for binding to the $tRNA^{Trp}$ (Doublie, et al., 1995), which could explain why the protein became so sensitive to proteolytic degradation and thus also explain its reduced abundance in the cells, as was observed by the SDS-PAGE/ESI-MS/MS experiments **(Supp. Figure S3).**

Supp. Figure S1-F

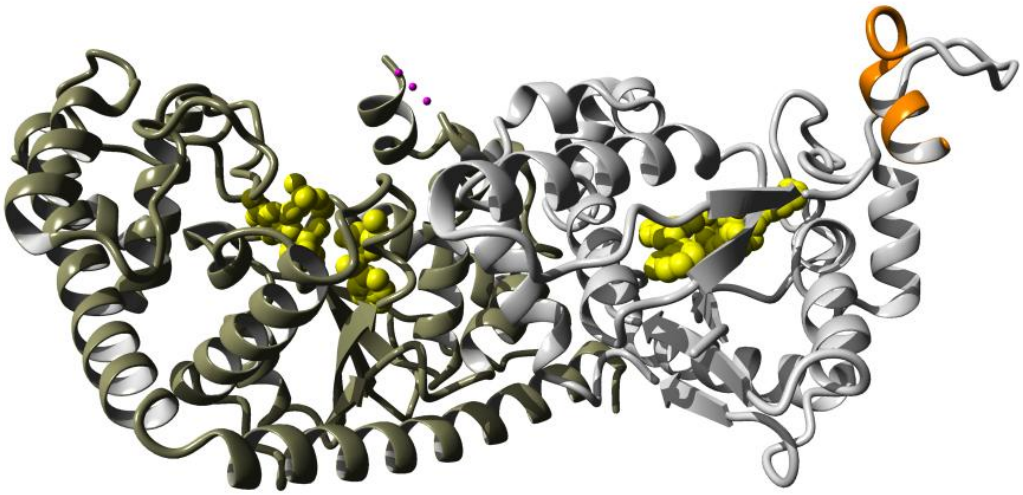

p.Pro266Argfs10X

The p.Pro266Argfs10X variant deletes several helical structures that are located on the outside of the protein, including the predicted anti-codon binding loop Ala-Gly-Arg-Ala-Gly starting at position 267 (Jia, et al., 2002), thereby affecting the enzyme's ability to bind $tRNA^{Trp}$. In addition, the frameshift variant may interfere with the dimerization of the protein. The low overall abundance of mtTrpRS protein in the fibroblasts of individuals I2 and I3 (**Supp. Figure S3**) suggest that the non-functional protein has a reduced stability, or, more likely, the mRNA encoding the truncated protein is degraded by nonsense-mediated decay.

Supp. Figure S1-G

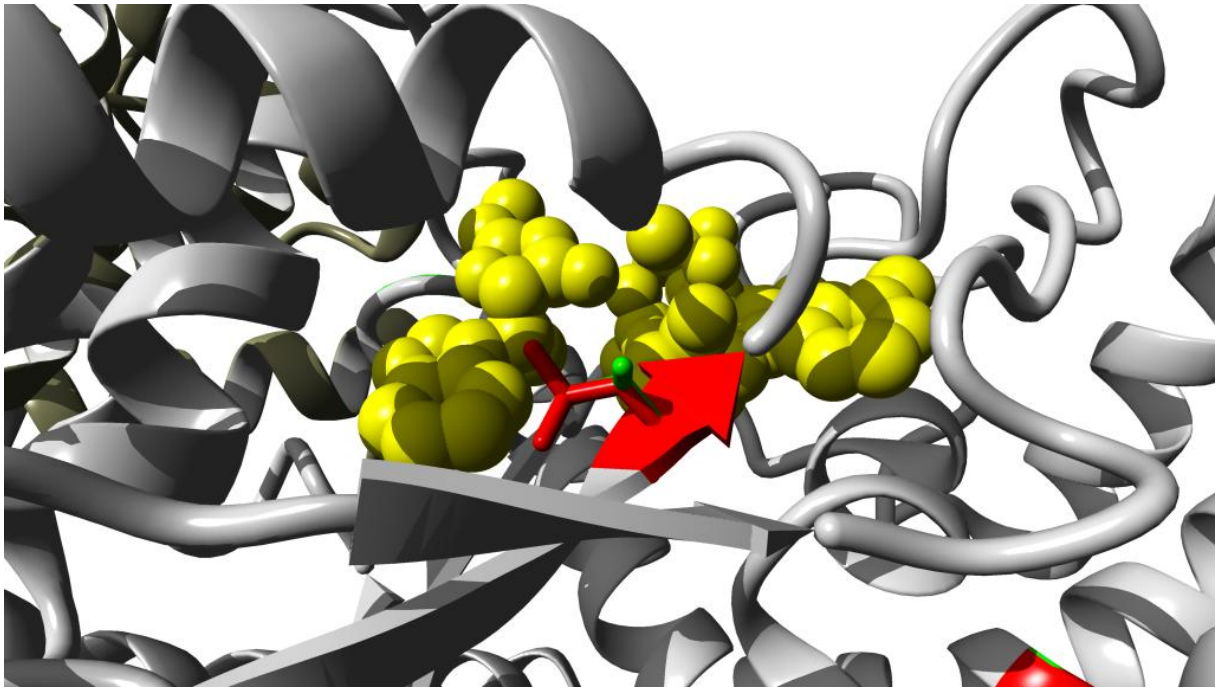

p.Val178Leu

The p.Val178Leu variant is located near the ligand binding pocket. Although the hydrophobicity of the region will remain similar, the size of the variant residue is larger and in order for this variant residue to fit the local conformation has to change, which is expected to affect the ligand binding properties of the protein.

Supp. Figure S2. MtTrpRS **protein expression abundance levels**

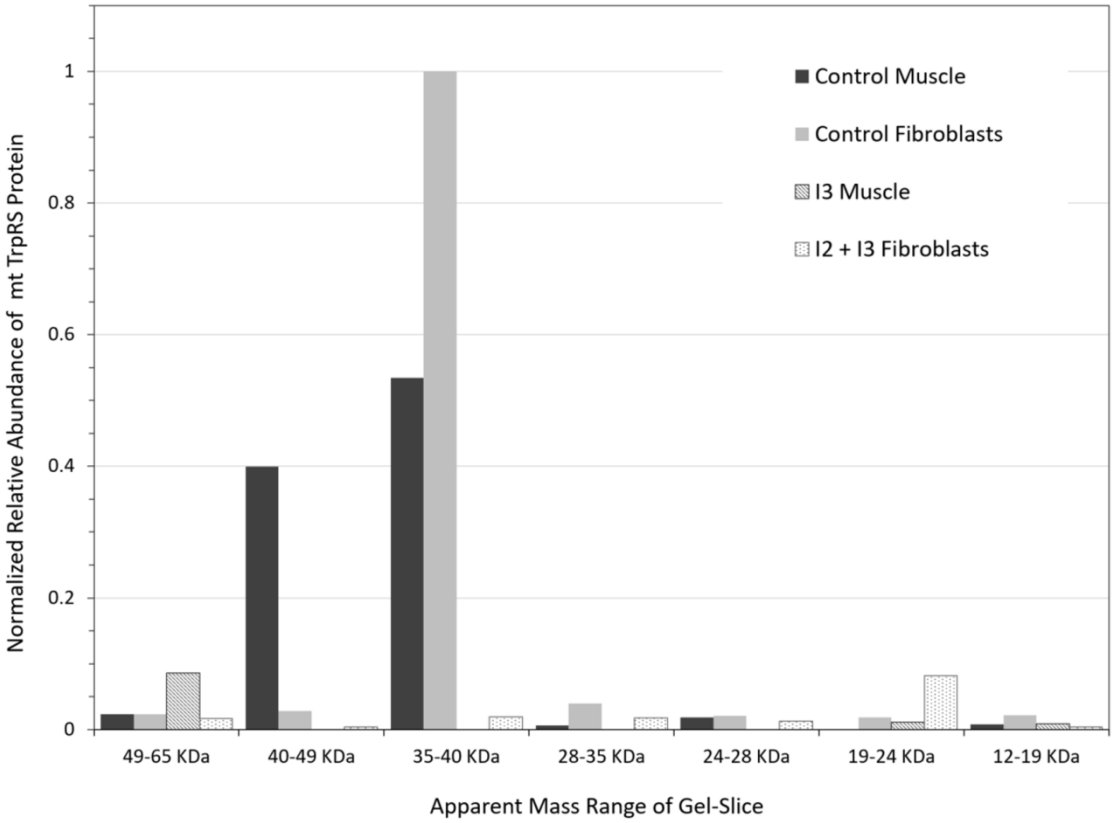

Supp. Figure S2 WARS2 (mtTrpRS) protein expression abundance levels are reduced in patient derived fibroblasts and muscle. The abundance of mtTrpRS was determined by ESI-MS/MS following in-gel tryptic digest of seven slices of a 12.5% Tricine SDS polyacrylamide gel covering an apparent mass range from 12 to 65 kDa. Protein identification and label free quantification was performed using MaxQuant (Cox and Mann, 2008). Main panel, relative IBAQ protein abundance values for mtTrpRS protein isoform 1 of each slice were normalized to the total abundance of VDAC1 in all slices and the value for the protein of control fibroblasts in th 35-40 kDa slice was set to 1. Values from two (control muscle, patient fibroblasts), three (control fibroblasts) or one (patient muscle) were averaged using four (patient fibroblasts) or two (all other samples) technical replicates each. For the control samples most of mtTrpRS protein was detected in the mass range from 35-49 kDa. Much smaller amounts were detectable in the patient samples at a wide range of masses indicating proteolytic degradation. Insert, sum of mtTrpRS abundance values of all slices from the main

panel renormalized by setting the value for control fibroblasts to 1. The overall detectable amount of mtTrpRS in patients was 7% for fibroblasts and 6% for muscle tissue compared to control.

Supplementary references

Cox J, Mann M. 2008. MaxQuant enables high peptide identification rates, individualized p.p.b.-range mass accuracies and proteome-wide protein quantification. Nat Biotechnol 26(12):1367-72.

Doublie S, Bricogne G, Gilmore C, Carter CW, Jr. 1995. Tryptophanyl-tRNA synthetase crystal structure reveals an unexpected homology to tyrosyl-tRNA synthetase. Structure (London, England : 1993) 3(1):17-31.

Jia J, Xu F, Chen X, Chen L, Jin Y, Wang DTP. 2002. Two essential regions for tRNA recognition in Bacillus subtilis tryptophanyl-tRNA synthetase. The Biochemical journal 365(Pt 3):749-56.

Yang X-L, Otero FJ, Ewalt KL, Liu J, Swairjo MA, Kohrer C, RajBhandary UL, Skene RJ, McRee DE, Schimmel P. 2006. Two conformations of a crystalline human tRNA synthetase-tRNA complex: implications for protein synthesis. The EMBO journal 25(12):2919-29.